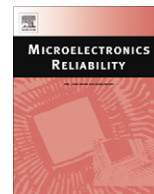




Contents lists available at ScienceDirect

Microelectronics Reliability

journal homepage: www.elsevier.com/locate/microrel

Simulation and experimental analysis of large area substrate overmolding with epoxy molding compounds

Thomas Schreier-Alt^{a,*}, Frank Rehme^{b,1}, Frank Ansorge^a, Herbert Reichl^c

^a Fraunhofer IZM, Micromechatronic Systems, Argelsrieder Feld 6, 82234 Oberpfaffenhofen, Germany

^b EPCOS AG, Anzingerstr. 11, 81671 Munich, Germany

^c Technische Universität Berlin, Fakultät IV – Elektrotechnik und Informatik, Gustav-Meyer-Allee 25, 13355 Berlin, Germany

ARTICLE INFO

Article history:

Received 6 November 2009

Received in revised form 19 August 2010

Accepted 13 October 2010

Available online xxx

ABSTRACT

This paper presents new experimental and numerical methods to characterize the transfer overmolding of substrates with epoxy polymer. We investigated Multi Chip Modules on ceramic panels as well as on printed circuit boards encapsulated as a Mold Array Package (MAP). Experiments show that the polymer flow during the overmolding process depends significantly on the mold height: While standard MAP-type mold cavities are filled homogeneously and symmetrically in most cases, low cavity heights (<500 μm) can cause the flow front to concentrate on a few flow paths (flow front fingering). We developed a numerical method to describe this inhomogeneous polymer flow. The reason for flow front fingering seems to be local variations of polymer viscosity which enforces a necking on distinct flow paths. Fingering can cause the formation of air traps and excessive wire sweep. We also developed new experimental methods to measure the pressure distribution within cavities: our sensor is based on commercially available, passive pressure sensitive films from FUJIFILM and is operational at temperatures up to 180°.

© 2010 Elsevier Ltd. All rights reserved.

1. Introduction: MAP-type overmolding

Transfer molding with epoxy molding compound (EMC) is a standard process for reliable chip encapsulation since decades. Currently the market trends clearly drive towards System in Package (SIP) [1]. They allow much higher component integration rates compared to classical single chip technologies. Additionally they have significant advantages for the manufacturers as they can offer complete functional modules to the OEM instead of single components, increasing the added value and uniqueness of their product. Its main advantage over pure front-end technologies is its flexibility of design by integrating discrete passive and active components within one package. Modules for mobile phones (Fig. 1) can integrate more than 50 components in a single package. In comparison with conventional solutions based on discrete components, the SIP solution reduces board space requirements by 95%.

One upcoming encapsulation standard for SIP can be identified to be the substrate overmolding process. The substrate to be overmolded typically is a Printed Circuit Board (PCB), a ceramic panel, a leadframe or a wafer [2,3]. The substrate consists of several electronic modules arranged in a MAP-type configuration. Each of

them is composed of numerous passive or active components. The assembled surface of the substrate is encapsulated by EMC and singulated by dicing. A simple tool for substrate overmolding and an overmolded PCB are pictured in Fig. 2. Details of molding tool and process are given at the end of this section.

Main advantages of these Mold Array Package (MAP-type) geometries for production are the following:

- One single mold tool can be used for multiple module dimensions as long as their height remains.
- Length of polymer flow can be minimized because runners for material supply can be omitted.
- Increased integration density of components within the mold tool leading to reduced packaging costs.

Typically the singulated modules are Quad Flat No Leads (QFN) or ball less package types. A very promising technology derived from ball less MAP-type molding is the embedded Wafer Level BGA (eWLB) approach [4,5]. Both encapsulation technologies, MAP-type molding as well as eWLB, combine the overmolding of large areas ($\varnothing = 25\text{--}100\text{ mm}$) with a relatively thin mold cover (height < 1 mm).

The MAP-type overmolding process of PCB substrates consists of several production steps: A substrate (labeled “1” in Fig. 2) and an epoxy pellet (inlet for pellet labeled “2”) are inserted into the mold tool (step A in Fig. 3). Both must be pre-heated, to

* Corresponding author.

E-mail address: thomas.schreier-alt@mmz.izm.fraunhofer.de (T. Schreier-Alt).

¹ Now at: Roche Diagnostics GmbH, Sandhofer Straße 116, 68305 Mannheim, Germany.



Fig. 1. Front-end module for mobile phones before encapsulation to a system in package.

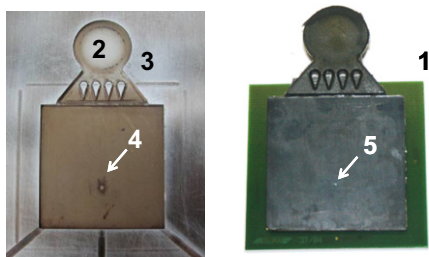


Fig. 2. Left: Molding steel tool. Label 2: Inlet for EMC pellet. Label 3: Film gate with shaping structures. Label 4: PZT cavity pressure sensor. Right: Overmolded FR-4 substrate with film gate. Label 1: Overmolded FR-4 substrate. Label 5: Mark of pressure sensor surface within EMC.

guarantee initial plasticity and flowability of the pellet. Pre-heating of the substrate increases thermal uniformity and adhesion between substrate and polymer. The pellet is crushed by a plunger, increasing thermal contact to the hot tool and melting (step B). After this preconditioning the plunger presses the polymer through the film gate and into the cavity on top of the PCB (step C). Specially designed shaping structures (labeled “3”) can be used to achieve sufficient shear heating within the EMC and a homogeneous flow front at the gate. After filling of the cavity the EMC is pre-cured for about a minute to guarantee sufficient gelation and therefore adequate contour accuracy during removal of the substrate (step D). In most applications the parts are post-cured after-

wards at the mold temperature for several hours. Our mold tool was equipped with a PZT pressure sensor from Kistler (labeled “4”). Small marks of the sensor can be seen on the overmolded substrate (labeled “5”).

The integration of sensors and actuators within MAP-type modules narrows the molding process window significantly, because their pressure sensitivity is much higher compared with monolithic silicon chips or passive components. Often the stress during the mold filling process can be neglected, considering the electronic part to be stress free at mold temperature. Consequently the simulation of thermo-mechanical stresses is restricted to temperature changes and subsequent failures like delaminations and popcorning [6,7]. Some research groups started to implement polymerization stresses into their models in order to investigate substrate warpage after molding [8–10]. Nevertheless there is the need to monitor also the pressure acting on the electronic parts during the polymer encapsulation process considering e.g. the spreading usage of MEMS sensors within automotive industry and their increased demand for signal stability, production tolerances and cost [11–13].

2. Simulation: Polymer flow during MAP-type overmolding

Numerical simulation of the polymer flow within MAP-type cavities is until now a challenging task for a process engineer. First the large amount of small gaps between electronic parts, mold wall and PCB has to be meshed precisely, heavily increasing the FEM computation time. Secondly, the filler particles within the polymer (up to 90 wt.%) can increase the flow resistance of the epoxy within small gaps and cause separation of filler and polymer matrix. Non uniform filler distribution can be a cause of failures such as cracks [14].

Commercially available tools for simulation of transfer molding are – as far as we know – not able to predict the filling behavior of polymers within thin (<500 μm), but wide-stretching gaps (>40 mm) precisely. Chen et al. [15] have observed viscosities of unfilled polymers within 200 μm wide gaps differing up to 75% from standard FEM predictions. Simulations mostly show a more or less symmetrical flow pattern around the gate which does not change significantly if one of the following parameters changes: filler degree, viscosity η , injection pressure p , temperature of the melted epoxy T or cavity height h . This fact can be seen in Fig. 4 where velocity distribution derived by standard FEM tools within gaps of 250 μm and 1000 μm thickness do not differ significantly from the Newtonian flow derived by Poiseuille’s theory. Fig. 5 shows that standard FEM simulations also show no difference in flow patterns when the mold height is reduced from 750 μm to 450 μm .

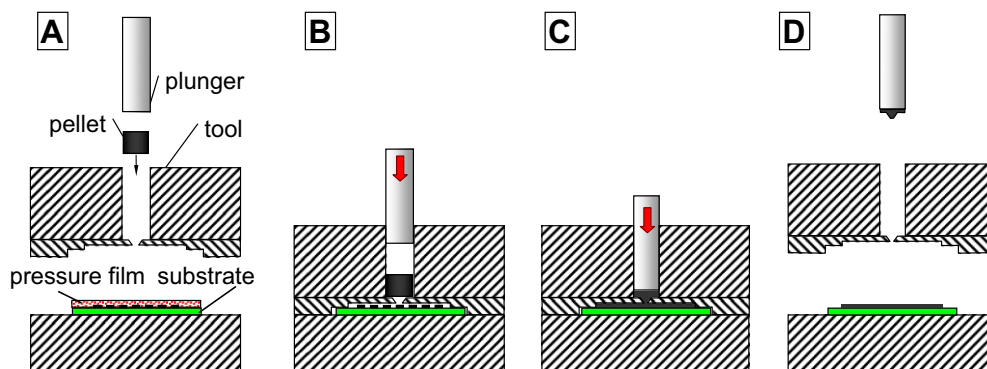


Fig. 3. Transfer molding process with central injection of the molding compound. Step A: Pellet and substrate are inserted into the mold tool and preheated. The substrate can be equipped with electronic components or a pressure sensitive film. Step B: The plunger presses on the pellet, the pellet melts. Step C: The melted polymer is pressed into the cavity. After filling the cavity the material is pre-cured for 2 min. Step D: The plunger is removed together with the cull. The substrate is removed.

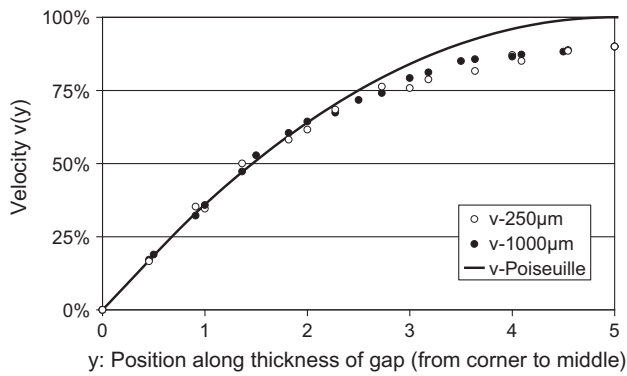


Fig. 4. Numerical (Moldflow MPI 3D) and analytical (Poiseuille) calculation of polymer velocity within gaps of 250 μm and 1000 μm .

The governing laws of polymer flow used by FEM models (Reactive Cross-Arrhenius-Macosco, Herschel-Bulkley-WLF) show no correction factors when narrow gaps are analyzed. Standard models without correction factors get definitely inaccurate if gap sizes are of the same dimension as the filler particles. The effect of temperature and filler degree on viscosity is theoretically described since the works of Einstein [16] as well as Ball and Richmond [17]. Our experiments indicate that the relation λ between maximum filler particle size $d_{\text{filler,max}}$ and gap size h is of significant influence on flow resistance. λ will be defined as:

$$\lambda = \frac{d_{\text{filler,max}}}{h} \quad (1)$$

To take into account the maximum filler size of a typical EMC (with 75–90 wt.% filler particles) we defined a corrected viscosity η^* . It depends on the geometrical parameter λ (described by a correction factor C) and material parameters typically used within Herschel-Bulkley-WLF or reactive viscosity models (temperature T , shear rate $\dot{\gamma}$, pressure p and fitting constants).

$$\eta^*(T, p, \dot{\gamma}, \lambda) = \eta_0(T, p, \dot{\gamma}) \cdot C, \quad (2)$$

$$C = \exp\left(\frac{2\lambda}{1-\lambda}\right).$$

The correction factor C was derived by fitting numerical simulations to our experimental results that will be described within Section 5. Until $\lambda = 0.4$ there is no significant difference between theories only considering interactions between particles and walls, e.g. the Bungay and Brenner model [18], and our fit. However for $\lambda > 0.5$ we get a much faster increase of viscosity with increasing filler to gap ratio (Fig. 6). The reasons are interaction forces between filler particles that have to be considered within highly filled

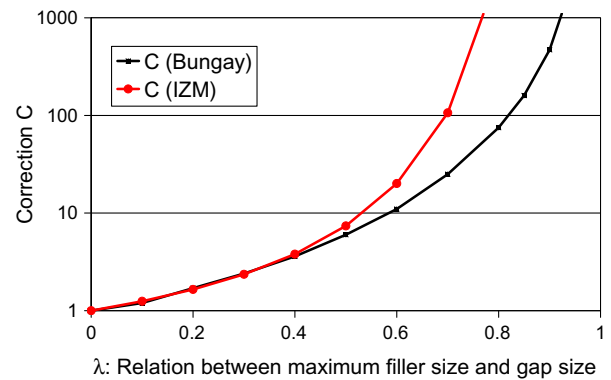


Fig. 6. Increase of C with increasing relation of maximum filler size against gap size.

epoxy molding compounds. These interactions increase flow resistance in narrow gaps much more than in wide cavities, especially for $\lambda > 0.5$ when only one maximum sized filler particle after the other can enter the gap and the whole filler distribution within the polymer matrix has to be rearranged.

3. Measurement of pressure distribution with sensitive films

In order to examine polymer flow behavior we measured the pressure within the cavity online by PZT pressure transducers mounted flushing with the mold cavity wall, chronologically recording pressure values at the measurement spot (labeled “4” in Fig. 2). Disadvantages of this sensor are the missing ability to record an areal pressure distribution and the occurrence of unattractive marks on the part’s surface (labeled “5” in Fig. 2). As the sensor’s mark can be even larger than one single singulated module, their usage within MAP-type transfer molding is rarely accepted. Another disadvantage of active sensors – electrical as well as optical – is that the signal transmission requires holes or grooves within the metal tool. This is undesirable, especially if the measurement should take place during the developmental stage only.

To overcome these disadvantages of conventional pressure sensors, a Prescale MW pressure sensitive film (sensitivity 10–50 MPa) from FUJIFILM [19] has been modified to enable its usage within transfer molding. Pressure sensitive films are based on a PET matrix that contains small microcapsules. Pressure upon the film causes the microcapsules to crack, starting a chemical reaction that is producing an instantaneous and permanent color change across the contact area. Pressure sensitive films record only the maximum pressure value applied on the film and are pressure sensitive up to 80 °C. To overcome the temperature restriction, we appended an

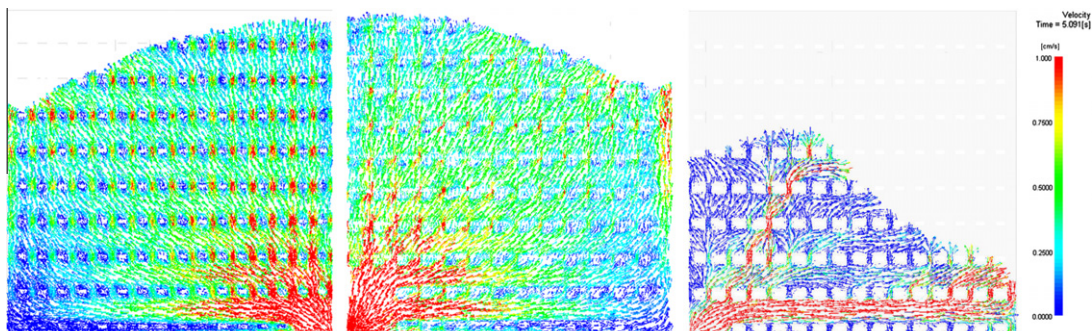


Fig. 5. Standard simulation of polymer velocities on substrates with a mold cavity height of 750 μm (left) and 450 μm (middle). No significant difference between the flow fronts can be observed. The picture on the right shows the polymer velocity after modification of the FEA tool by using a corrected viscosity η^* according to formula (2).

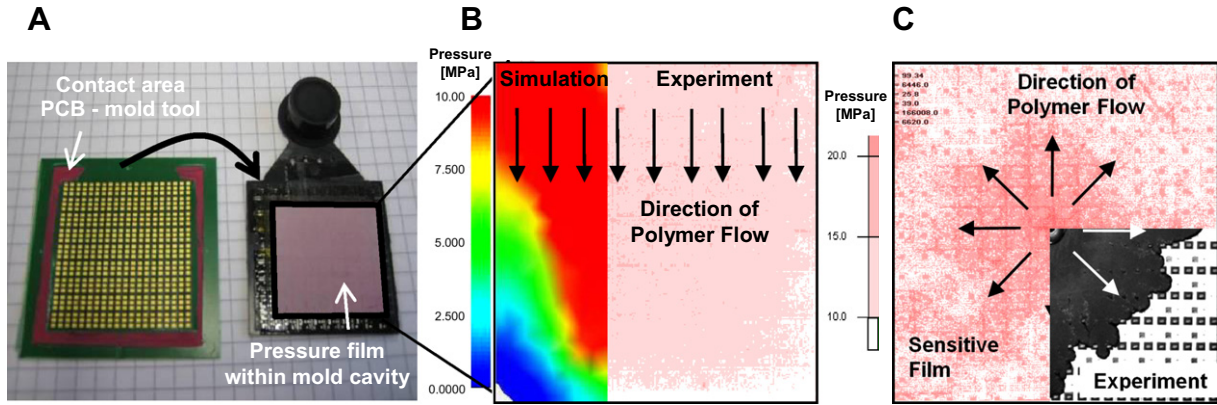


Fig. 7. A: PCB with imprints of the mold tool and removed EMC with pressure sensitive film. B: Pressure distribution of a film gate by simulation (left) and sensitive film. C: Pressure distribution of a central pin gate by pressure film and short shot experiment (Fujifilm Prescale data analysis by “Fujifilm Pressure Distribution Mapping System PFD-8010E”).

isolating polyimide coating and an adhesive layer onto the film. We mounted this multilayer on top of the PCB in such a way that the liquid molding compound is flowing over the multilayer (Fig. 3). As the softening temperature of the PET resin within the Prescale film is 80 °C, the additional layers have to guarantee that the cavity pressure is almost entirely transferred to the pressure sensitive particles within the Prescale film. For examination of the color change, the substrate can simply be separated from the adhesive film of the multilayer (Fig. 7A). Also the adhesion between EMC and PI film is weak enabling their separation. The color intensities of the separated pressure sensitive film is analyzed by a commercial scanner and transferred into a color spectrum by software. With our multilayer film we can enable test durations at 180 °C of several minutes without detracting of the sensor function.

The first process under investigation is an FR-4 board overmolded with EMC through a film gate as shown in Fig. 2. The polymer melt has been injected directly onto a Prescale-IZM-multilayer mounted onto the PCB within the cavity. The color distribution on the FR-4 board (Fig. 7B) is very homogeneous with a slight pressure drop with increasing distance from the gate. The pressure distribution is in accordance with numerical simulations, which expect slightly lower values than measured (~10% deviation).

The pressure values captured by the multifilm measurement technique have been compared with values from piezoelectric pressure sensors mounted within the same mold tool. Apart from FR-4 substrates we tested the technology with ceramic substrates (Fig. 7C) and used different transfer molding machines with different positions of the PZT sensor. We derived a semi-empirical formula that describes the sensitivity S of the pressure sensitive film at temperature T and pressure p . For transfer molding with $T \approx 175$ °C and $p \approx 5.7$ –12.5 MPa the following linearization was used for pressure derivation.

$$S = \frac{p_F}{p} = \left(1 - \frac{T - T_{AB}(RH_{0\%})}{\Delta T(T)} \cdot \frac{\Delta p(p_F, T)}{p_F} \right)^{-1} \approx \left(1 - \frac{T - 115 \text{ °C}}{35 \text{ °C}} \cdot \frac{2.5 \text{ MPa}}{p_F} \right)^{-1} \Big|_{175 \text{ °C}, 10 \text{ MPa}} \quad (\text{linearization}) \quad (3)$$

where p_F is the pressure measured by the Prescale film and p is the real pressure, e.g. recorded by the PZT sensor. $T_{AB}(RH_{0\%})$, $\Delta T(T)$ and $\Delta p(p_F, T)$ are material specific values derived from experiments. The measured values of p_F do not necessarily represent the maximum pressure distribution at the beginning of the post pressure as the sensitivity S depends on temperature which can change during the transfer molding process. Therefore the time dependent thermal behavior on the substrate’s surface should be regarded. Numerical simulations are advantageous because they also give a rough value for the expected pressures and simplify the correct choice of Prescale film. In most cases, with a proper pre-heating of the substrate and the polymer pellet, the temperature remains constant and the Prescale color pattern will represent the maximum pressure distribution.

The maximum pressure values have been varied between 5.7 MPa and 12.5 MPa. The measurement values of the PZT pressure sensors are displayed in Table 1 and compared with the multilayer film values. The percentage values refer to the multilayer values in relation to the PZT sensor. We found both values to agree

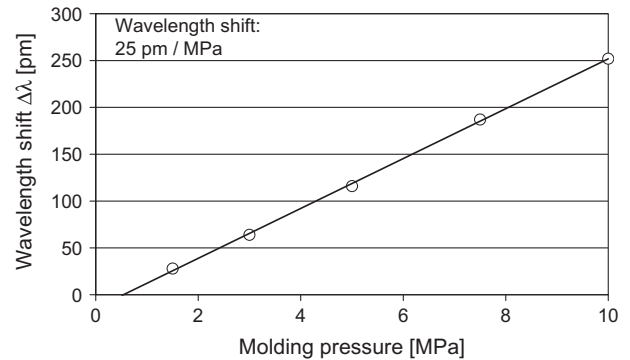


Fig. 8. Wavelength shift of a fiber optic pressure sensor with increasing molding pressure.

Table 1

Relation of cavity pressure values recorded during transfer molding by multilayer film “p (film)” in relation to values of standard PZT pressure sensors from Kistler “p (PZT)”.

p (film)/ p (PZT)	$p = 5.7$ MPa	$p = 7.5$ MPa	$p = 8.5$ MPa	$p = 9.0$ MPa	$p = 12.5$ MPa
Sensor near gate	100%	97%	105%	90%	98%
Sensor far away from gate	102%	104%	102%	98%	98%

within $\pm 10\%$, which is also in accordance with the finite element analyses performed by Autodesk Moldflow 3D.

In order to control the pressure distribution during transfer molding also within mass production, the authors invented a new in-mold measurement method. Basic principle of the invention is to monitor the polymer pressure on the substrate by adjacent fiber optic Bragg gratings (patent pending). The wavelength of the light reflected at the grating depends linearly on the molding pressure (Fig. 8). As it also depends on the temperature, methods for temperature compensations have to be taken [11]. Main advantage of the new sensor is its ease of integration and the time dependent measurement of the areal distribution by the fiber optic sensor network (multiplexing of dozens of Bragg sensors within one fiber).

4. Experiments: MAP-type overmolding of FR-4 substrates

The flow behavior of polymers on Multi Chip Module (MCM) substrates is far more complicated than the classical single chip encapsulation. Even on small FR-4 substrates (edge length: 25 mm) without any assembled components surprising results can be observed. Fig. 9 shows the progress of EMC during substrate overmolding by subsequent short shots. They have been produced by increasing the amount of EMC material within the plunger step by step. The flow front splits into two separate flow paths shortly after injection into the cavity (state A). First, the material flows uniquely along the edges of the cavity. Then an additional flow path starts in the centre of the substrate (B and C), but keeps sharply separated from the boundary flow paths. They reach the PCB corner opposite of the gate slightly before the central flow path and continue their way along the cavity border (D). If the cavity is not evacuated the enclosure of air traps is unavoidable (E).

The reason for this behavior is rooted in the reduced stiffness of the substrate above its glass transition temperature. As the coefficient of thermal expansion (CTE) is rising sharply above T_g even small temperature differences between the mold tool ($\sim 175^\circ\text{C}$)

and the PCB cause a significant elongation of the substrate after closing of the mold tool. In this case the substrate is mechanically fixed between the halves of the mold tool and the elongation of the substrate leads to a convex, \cap -shaped bending and forces the polymer to flow around this central elevation. With increasing pressure at the gate and further increasing temperature of the substrate, buckling of the PCB starts in the middle leading to a \cup -shaped substrate with three distinct flow paths. This curvature of the substrate can still be measured after ejection, because its shape is frozen by the cured epoxy polymer. If the experiment is conducted with a substrate assembled with electronic components, the warpage is suppressed by the components (Fig. 10). They work as spacers between PCB and mold tool and are preventing the soft substrate to buckle by mechanically touching the upper mold tool. This can be demonstrated by short shots: the highest components on the board are not covered by EMC but exposed.

A reliable way to prevent the buckling of the PCB is to use substrates with reduced thickness. Without being rigidly clamped between the two mold tools the substrate can slightly slip through them during elongation. The disadvantage of this method is the possibility of polymer flash (Fig. 10).

5. Discussion: Comparison between experiments and simulation of MAP-type overmolding

Our experiments show another important effect during MAP-type overmolding that is not predicted correctly by standard numerical simulation software, because an appropriate flow model is not implemented up to now. Overmolding with a film gate produces a straight flow front that is moving over the panel. We have analyzed this for flow path lengths up to 40 mm. Experiments with evacuated molds with pin gates show that the straight flow front starts to ripple after ~ 20 mm (Fig. 11). These flow front instabilities can also be observed on plane substrates without any assembled components, which is especially important for overmolding

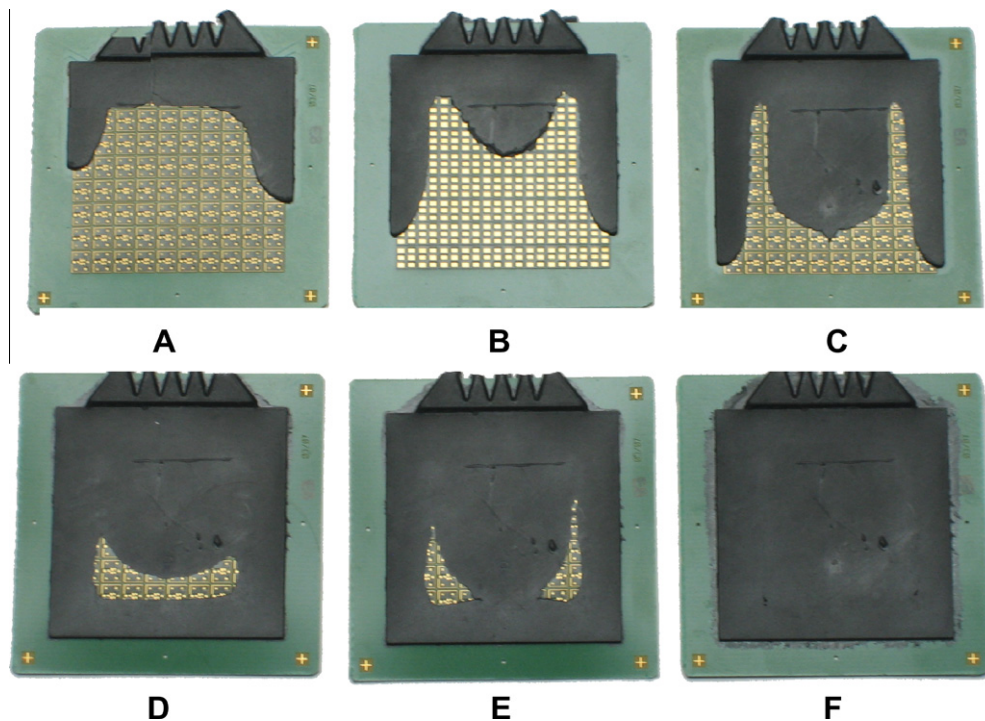


Fig. 9. The filling behavior of EMC on an FR-4 substrate without components can be surprisingly complicated which can be illustrated by short shots.

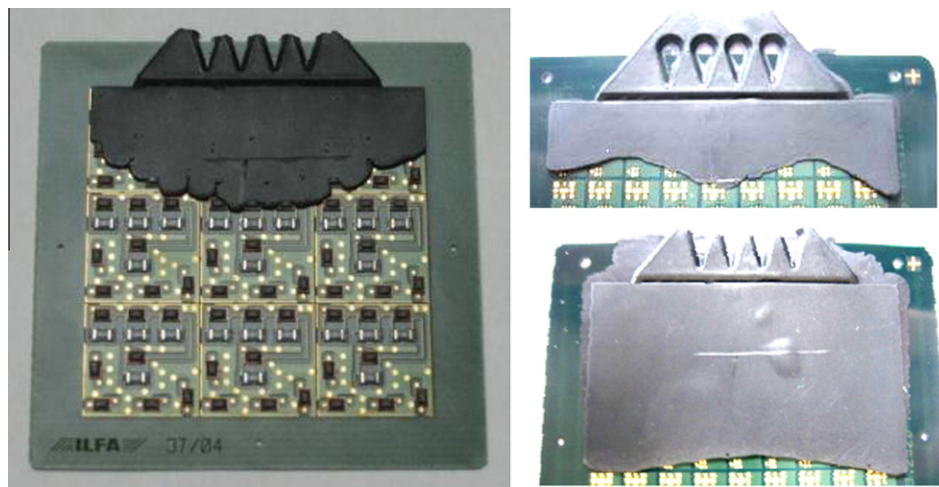


Fig. 10. Left: Short shot of PCB overmolding with assembled components. Right: PCB with reduced substrate thickness shows homogeneous, straight flow front.

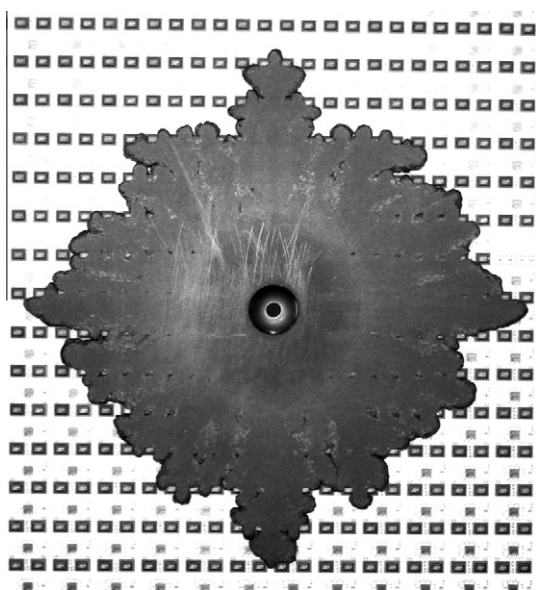


Fig. 11. Flow of highly filled EMC over an assembled ceramic panel, injected with a pin gate.

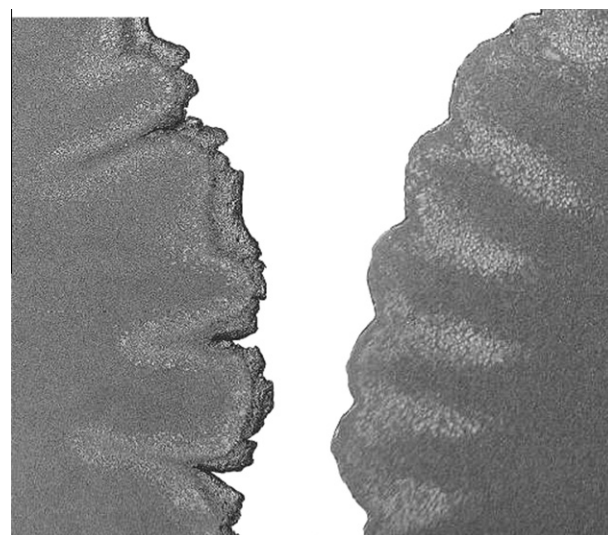


Fig. 12. Short shots with an EMC with filler cut $53\ \mu\text{m}$ (left) and with filler cut $45\ \mu\text{m}$ (right). Different intensities of flow front fingering can be observed. Both polymers had a filler content of 90 wt.%.

of large wafers (Fig. 12). Table 2 gives dimensions of the cavities used within the experiments.

This behavior is called “flow front fingering instability” within the literature. Within filled polymers, this effect can be caused by local variations in filler concentration (e.g. agglomerations) that locally change the viscosity [20]. The effect has also been reported with unfilled shear thinning viscoelastic fluids [21]. Here, the flow front should get smoother if the filling velocity is lowered in such a way that the polymer is always in the Newtonian range. Without the shear thinning effect no inhomogeneities should appear. Because of the fast polymerization of our material, we were not able to lower injection speed sufficiently to observe this effect. Flow front fingering can also be observed when the advancing flow front is increasing in length, e.g. when spreading symmetrically from a pin gate. The occurrence of this effect seems to be linked to shear stresses perpendicular to the flow direction [21]. If a pin gate is used, the velocity of the melt decreases monotonously with increasing distance from the gate. Consequently the shear rate at the spreading flow front decreases steadily until the Newtonian re-

Table 2

Geometry of the cavities.

Length	100 mm
Width	100 mm
Height	0.45 mm and 0.55 mm
Pin gate diameter	2 mm
Pin gate position	Centre

gime is reached (if applicable), where shear rate will be independent from the polymer’s viscosity (Fig. 13). Until this point small variations in shear rate $\dot{\gamma}$ can change the viscosity of the material. This shear thinning effect is typically used when the polymer is forced through the narrow mold gate. A similar effect can happen when the material is forced to flow through narrow gaps between components. This locally increased shear rate increases flowability within these regions and leads to a necking of the flow to few distinct paths with reduced viscosity. Consequently the circular flow front splits up into several flow paths. Little random variations of polymer velocity seem to be enough to break the symmetry of

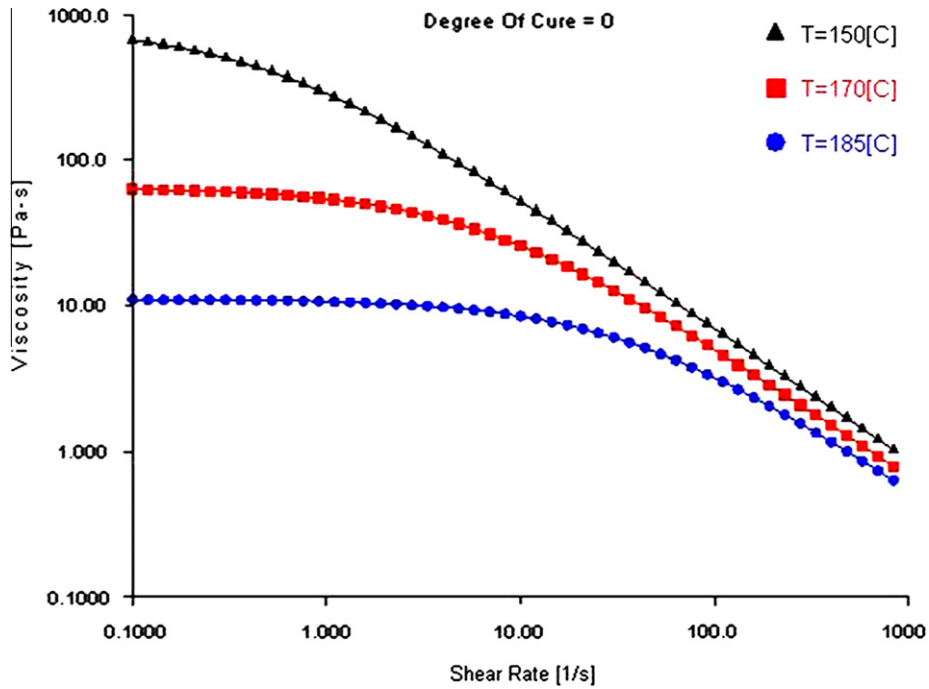


Fig. 13. Viscosity of ShinEtsu KMC-184 with Newtonian regime $\dot{\gamma} < 5 \text{ s}^{-1}$ and non-Newtonian regime $\dot{\gamma} > 5 \text{ s}^{-1}$.

the filling behavior. At the contact area of the separate flow paths a weld line is formed where unfilled voids remain.

The inhomogeneous filling behavior has been observed in short shots, where we stopped the overmolding process during the flow to inspect the flow front. It has to be mentioned that the filling pattern of a short shot might change after the injection pressure is removed. However, we were able to correlate an inhomogeneous polymer flow with the occurrence of small voids (diameter $>200 \mu\text{m}$ on the polymer surface, examined by visual inspection) of completely overmolded substrates.

It could be demonstrated, that the following parameters contribute to the occurrence of flow front fingering instabilities:

- Decreasing thickness of overmolding.
- Decreasing distance between electronic parts and between parts and mold wall.
- Increasing viscosity of the polymer.
- Increasing size of the filler particles.

This fingering of the flow front during transfer molding can not easily be implemented into standard transfer molding simulation tools. Based on the thixotropic index [22], we numerically adjusted the material behavior by a thixotropic shear thinning parameter that is highest at the gate location and monotonically drops with proceeding time. Not only could the detailed form of the flow front

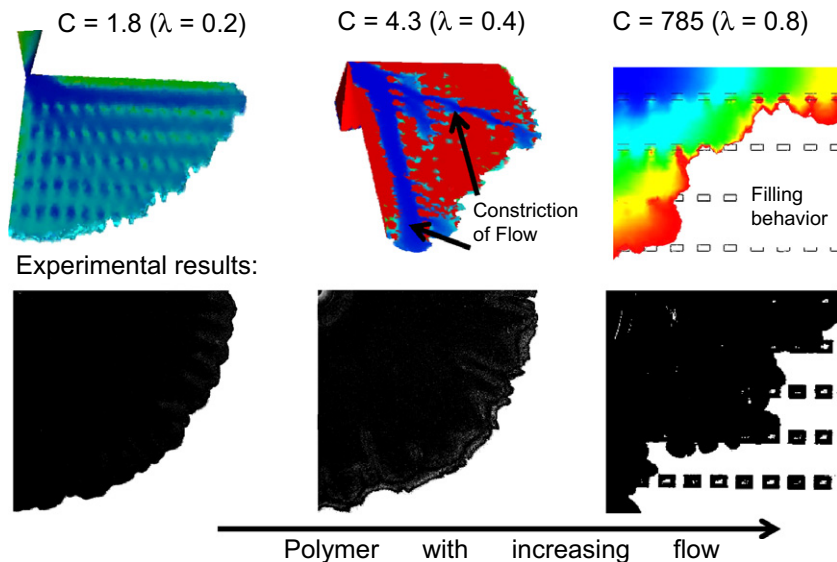


Fig. 14. Simulation of filling behavior on a substrate with successively increasing filler/gap relation (left: filler cut $45 \mu\text{m}$ with silicone additives, middle: filler cut $53 \mu\text{m}$ without additions, right: substrate with components and locally reduced gap sizes).

be predicted, but also the locally reduced viscosity within a few preferred flow paths between the components (Fig. 14). At the beginning of overmolding the regions with slow material movements are additionally provided with molten resin by the neighboring preferred flow paths, but the occurrence of these shear thinned regions seems to be already the forerunner of an asymmetrical filling behavior where regions far away from the flow paths remain unfilled.

6. Summary

Homogeneous material flow and pressure distribution within the cavity is of particular importance for encapsulation of mechanically sensitive parts, e.g. MEMS. With the use of pressure sensitive films a fast and inexpensive estimation of the pressure distribution can be achieved. Our multilayer film design is based on commercially available color changing papers (e.g. Prescale), an adhesive layer and an isolating film. This assembly enables tests for several minutes at 180 °C without detracting of the sensor function. The accuracy of this pressure measurement method is ~10%, checked by conventional pressure sensors located at different positions within the mold walls. The pressure results are also fitting well with numerical simulations.

By using a standard molding process, the polymer melt has been injected directly on this multilayer, generating red color changes on the Prescale film depending on the local maximum pressure value. Also the contact pressure between solder pads and bottom mold wall could be measured with the pads emerging clearly from the flat PCB surface.

We could clearly distinguish two different kinds of flow behavior during MAP-type overmolding: 1. Homogeneous filling of the cavity with a closed flow front and a continuous pressure drop along the flow path. 2. Contraction of the polymer flow within few, narrow paths with increased shear rate, reduced viscosity and excessive velocity.

Additionally we could show that modifications of the computational fluid simulation tool increase the accuracy of the flow behavior prediction, especially of the filling patterns with concentrated flow paths. The models have been validated with short shots within the transfer molding machine.

Acknowledgement

We would like to thank Ralf Andussies from FUJIFILM Recording Media GmbH for valuable support concerning measurement strategies at elevated temperatures. The authors wish to thank VDI/VDE-IT, especially R. Schliesser for their financial support.

References

- [1] Ardebili H, Pecht MG. Encapsulation technologies for electronic applications. Elsevier; 2009.
- [2] Marengo N et al. Investigation of key technologies for system-in-package integration of inertial mems. In: Symposium on design, test, integration and packaging of MEMS/MOEMS; Rome, Italy: 1–3 April, 2009.
- [3] Falat T et al. The influence of process parameters and materials properties on stress distribution in MEMS – ASIC integrated systems after molding – numerical and experimental approach. In: International conference on thermal, mechanical and multi-physics simulation and experiments in micro-electronics and micro-systems, EuroSimE 2009, Delft, The Netherlands; 2009.
- [4] Plieninger R, Dittes M, Pressel K. Modern IC packaging trends and their reliability implications. *Microelectron Reliab* 2006;46(9–11):1868–73.
- [5] Meyer T, Ofner G, Bradl S, Brunnbauer M, Hagen R. Embedded wafer level ball grid array (eWLB). In: Proceedings of the 2008 electronic packaging technology conference (EPTC), Singapore, December 9–12; 2008. p. 994–8.
- [6] Lall P, Pecht M, Hakim EB. Characterization of functional relationship between temperature and microelectronic reliability. *Microelectron Reliab* 1995;35(3):377–402.
- [7] Gannamani R, Pecht M. An experimental study of popcorning in plastic encapsulated microcircuits. *IEEE Trans Compon, Packag, Manuf Technol – A* 1996;19(2):194–201.
- [8] Jansen KMB et al. Modeling and characterization of molding compound properties during cure. *Microelectron Reliab* 2009;49(8):872–6.
- [9] de Vreugd J, Jansen KMB, Ernst LJ, Bohm C. Prediction of cure induced warpage of micro-electronic products. *Microelectron Reliab* 2010;50(9):910–6.
- [10] Kim YK, Park IS, Choi J. Warpage mechanism analyses of strip panel type PBGA chip packaging. *Microelectron Reliab* 2010;50(9):398–406.
- [11] Schreier-Alt T, Ansoerg F. Process optimization: throwing light on electronics encapsulation. *Kunstst Int* 2009;99(6).
- [12] Müller-Fiedler R, Knobloch V. Reliability aspects of microsensors and micro-mechatronic actuators for automotive applications. *Microelectron Reliab* 2003;43:1085–91.
- [13] Feiertag G, Winter M, Leidl A. Packaging of MEMS microphones. In: Proceedings of the 2009 SPIE Europe international symposium on microtechnologies for the new millennium, Dresden; May 4–6, 2009.
- [14] Huang Y, Bigio D, Pecht MG. Fill pattern and particle distribution of underfill material. *IEEE Trans Compon Packag Technol* 2004;27(3):493–8.
- [15] Chen SC et al. Preliminary study of polymer melt rheological behavior flowing through micro-channels. *Int Commun Heat Mass Transfer* 2005;32:501–10.
- [16] Einstein A. Eine neue Bestimmung der Moleküldimensionen. *Annalen der Physik* 1906;324(2):289–306.
- [17] Ball RC, Richmond P. Dynamics of colloidal dispersions. *Phys Chem Liq* 1980;9(2):99–116.
- [18] Bungay PM, Brenner H. The motion of a closely fitting sphere in a fluid-filled tube. *Int J Multiphase Flow* 1973;1(1):25–56.
- [19] <http://www.fujifilm-prescale.eu/>.
- [20] Becker KF, Vollbrecht H, Braun T, et al. Basic design guidelines for a robust underfilling process. In: Proceedings of the international acousto microscopic imaging symposium – IAMIS 2000, 19–20.10.00, San Jose, CA, US.
- [21] Kabanemi K, Hétu JF. Elastic flow-front fingering instability in flowing polymer solutions. *Rheol Acta* 2006;45(5):693–704.
- [22] Okuno A et al. Properties and reliability of liquid epoxy resin for LSI fabrication with the printing encapsulation system (PES). *Electron Commun Jpn*, 2 1997;80(2):431–9.